Biuletyn WAT
Vol. LXVII, Nr 3, 2018

Analysis of steel-reinforced high-strength concrete deep beam displacement under dynamic loads

WALDEMAR CICHORSKI

Military University of Technology, Faculty of Civil Engineering and Geodesy,
Department of General Construction, ul. Gen. Witolda Urbanowicza 2,
00-908 Warsaw, Poland, waldemar.cichorski@wat.edu.pl

Abstract. The paper presents an analysis of the deformation of a dynamically loaded rectangular reinforced-concrete deep beam, including the physical nonlinearity of construction materials: concrete and reinforcing steel. The solution was acquired with the use of the method presented in [15]. The displacement of three plate types under various loads, up to dynamic load capacity depletion, was analysed. The results of numerical solutions are presented, with particular emphasis on the impact of the very high strength of concrete and steel on the reinforced concrete plate displacement. The work confirmed the correctness of the assumptions and deformation models of concrete and steel as well as the effectiveness of the methods of analysis proposed in the paper [1, 15] for the problems of numerical simulation of the behaviour of reinforced concrete deep beams under dynamic loads.
Keywords: mechanics of structures, reinforced concrete structures, deep beams, dynamic load, physical nonlinearity
DOI: 10.5604/01.3001.0012.6612

1. Introduction

The aim of the work is the analysis of the influence of very high strength of concrete and reinforcement steel on the performance of rectangular reinforced concrete deep beams loaded dynamically with the inclusion of the physical nonlinearity of the construction materials: concrete and steel. The deep beam deformation was analysed with respect to the variation of vertical displacements in the three beam types under various loads, up to dynamic load capacity depletion. The solution was acquired with the use of the method of analysis of non-elastic behaviour of the reinforced dynamically loaded concrete deep beam [15].

The essence of this method consists of the following elements: dynamic modelling of the material properties, modelling of the process of deformation of the flat construction framework – reinforced concrete deep beam, and also algorithmisation and numeric programming of the solution. Modelling of the properties of the construction materials was carried out with the use of the assumptions of flow plasticity theory. The model of plastic/ideally viscoplastic material was used for the reinforcement steel, taking into account the plastic retardation effect. Modelling the dynamic properties of concrete was a topic of consideration for many publications, i.e. [9, 18]. Constitutive modelling of high-value and ultra-high-grade concrete properties was the subject of study in [8]. For concrete, a non-standard model of dynamic deformation was adopted in [4,14]. This model describes the elastic properties of concrete, the limited properties of ideal viscoplasticity on the initial dynamic surface of plasticity, material weakening and volume changes. The degradation of the deformation module was ignored in the model. The adopted concrete model facilitates a simplified description of material scratching or crushing as states of loss of load capacity achieved in the process of material weakening. A reduced form of the dynamic concrete model [14] was adopted in the study, reduced to the state of flat stress, both for loading and unloading processes. The limit curve for the adopted concrete model is shown in Fig. 1.

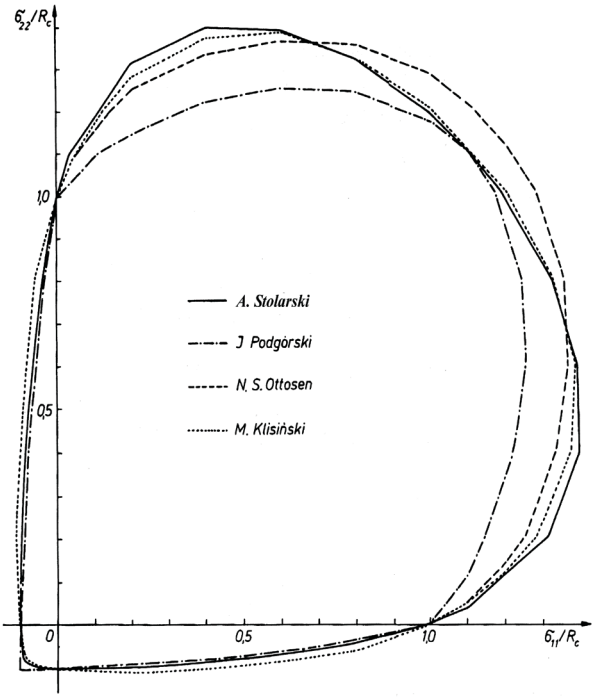

Fig. 1. Limit curve for the adopted concrete model [14] in a flat stress state

Achieving the goal required the introduction of constant properties into the adopted concrete model, allowing the description of the properties of concrete of very high strength. An assumption was adopted, in the modified concrete model, that the boundary deformation values may be variable and dependent on the class of concrete [1, 16]. The analysis method of the effort of the construction form was formulated with the use of the principles of the finite element method [5]. For the reinforced concrete deep beam, treated as a composite material consisting of the concrete matrix strengthened with thin rods of steel reinforcing, a hypothesis for the cooperation of the reinforcing rods and matrix material was proposed. The solution of dynamic systems of the displacement equations for the displacement of the finite element method was conducted based on algorithms and programmes of numerical analysis of the flat tension state, which allows the identification of the states of displacement, strain, strain rate, and stress with the inclusion of the effects of physical material nonlinearity, including concrete scratching.

In this study, the results of numerical solutions for the reinforced concrete deep beam are presented, which was the topic of the static experimental research of F. Loenhardt and R. Walter [6]. The study describes the diversified process of dynamic stress/strain and deformation of a reinforced concrete deep beam in relation to the very high strength concrete grade. The impact of the very high concrete and reinforcing steel strength on the dynamic load capacity of reinforced concrete beams was analysed, taking into account the physical non-linearities of the construction materials.

2. Subject of the analysis

The subject of the analysis are deep beams made of concrete matrix strengthened with thin, steel reinforcement rods in an orthogonal arrangement. The deep beam is loaded on the upper edge with a constant-over-time and equally distributed dynamic load $p(x,t) = p = \text{const}$.

An analysis of damage to various types and sizes of beams made of high-grade concretes was discussed in [4, 11, 12].

A numerical analysis was applied to a rectangular reinforced concrete deep beam with orthogonally arranged reinforcement, designated in the paper of F. Leonhardt and R. Walther [6] as WT3, fig. 2. The deep beam was the subject of the analysis in paper [2, 7].

The dimensions of the deep beam are: length, breadth: $L = B = 160$ cm, thickness: $t = 10$ cm. The main reinforcement of the deep beam was made in the form of 4 layers of reinforcement loops with a yield point of $f_y = 410$ MPa and a rod diameter of $\phi 8$, placed in the lower part of the deep beam. The remaining part of the deep beam is reinforced with vertical and horizontal stirrup reinforcement made of steel

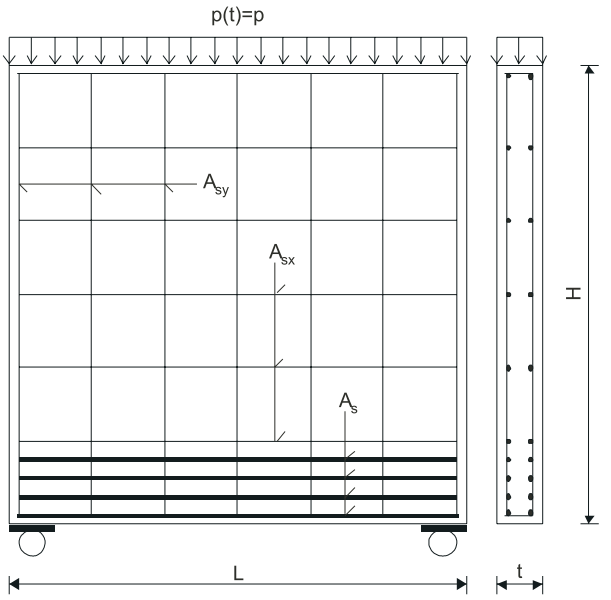

Fig. 2. Reinforced concrete deep beam diagram

with a yield point of f_y = 240 MPa, a rod diameter of ϕ5, and spacing of 26 cm. The concrete matrix was made of concrete with the compression strength of f_c = 30 MPa and an elongation strength of f_t = 3 MPa.

Taking into account the use in the numerical construction analysis of high strength concrete, paper [17] included a proposed modification of the concrete deformation model. The essence of the proposed modification of the concrete model is a change in the interpretation of the size of boundary deformation ε_{fc} for the phase of ideal viscoplasticity and ε_{uc} for the phase of material weakening. In the basic version of the model, on the basis of the analysis of the results of experimental research, boundary deformations ε_{fc} are determined as constant values for a single--axis compression of 2‰, regardless of the concrete class, whereas for boundary deformations ε_{uc}, the values were determined within the range of ε_{uc} = (6 - 12) ‰, on the condition that lower values of ε_{uc} may be used for concrete of higher class, and higher values of ε_{uc} for concrete of lower and medium class, but without the exact designation of the relation with the concrete class. Currently, in the modified concrete deformation model, it is assumed that the boundary deformation values ε_{fc} and ε_{uc} may be variable and dependent on the concrete class, in accordance with the concrete strength variability function specifying the so-called strength indicator, as described in paper [17].

As a consequence, material properties describing the constitutive concrete model, shown in table 1, were adopted for the numerical analysis.

Table 1

Boundary parameter values describing the concrete model

Concrete grade	f_c [MPa]	f_t [MPa]	ε_{ec} [‰]	ε_{fc} [‰]	ε_{uc} [‰]	E_c [GPa]
C30	30.	3	1.20	2.00	12.00	25.0
C100	100	10	2.08	2.80	11.25	48.0
C200	200	20	3.88	4.49	10.71	51.50
C300	300	30	5.71	6.21	10.21	52.5

A graphic interpretation of the material parameters describing the constitutive concrete model is shown in Fig. 3, in the plane of stresses and deformation for single-axis compression. In this picture, the Ψ_d indicator describes the dynamic strength of the concrete in accordance with the model described in the paper [14].

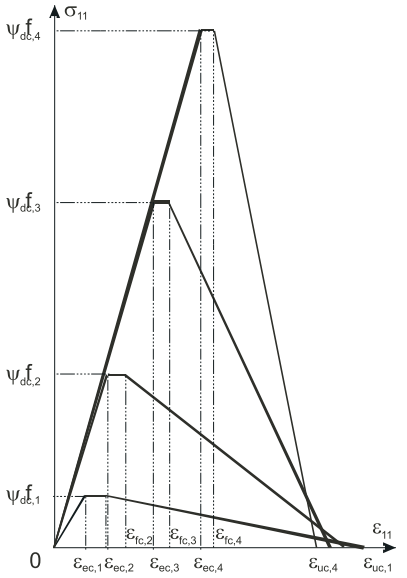

Fig. 3. Graphic interpretation of the material parameters of the constitutive concrete model.

For increased steel strength, a modification was made to the steel strength parameters of the main reinforcement of the deep beam, i.e. rods with a diameter of ϕ8. The modification involved using steel class *A – H* with a yield point of f_y = 690 MPa.

The intensity of dynamic load designates the dimensionless parameter $\alpha = P/P_0$ of auxiliary, total load of the deep beam $P_0 = p \times L$, in relation to the level of static deep beam carrying capacity P_0. Assessment of the level of static deep beam carrying capacity in relation to each deep beam type, in accordance with [3], amounts to:

— for C100, C200, C300 concrete and A-III steel: P_0 = [2210 kN/2595 kN/3317 kN]
— for C100, C200, C300 concrete and A-H steel: P_0 = [2085 kN/3028 kN/3999 kN].

3. Analysis of reinforced concrete deep beam displacement

To illustrate the impact of high-strength concrete on the diversified process of dynamic stress/strain and deformation of rectangular reinforced concrete deep beams, numerical experiments were carried out for a beam with the reinforcement arranged like in experiment [6] and with modified parameters describing the constitutive model of concrete (concrete grade *C100, C200, C300*). Additionally, the impact of changing the strength parameters of the reinforcing steel, i.e. the impact of swapping *A-III* regular steel, similarly to experiment [6], for *A-H* steel with increased strength, was analysed.

For that purpose, the following points in the central section (designated in fig. 4) were adopted for the observation of dynamic changes of displacement of the deep beam: x_d — lower edge, x_s — half beam height x_g — upper edge.

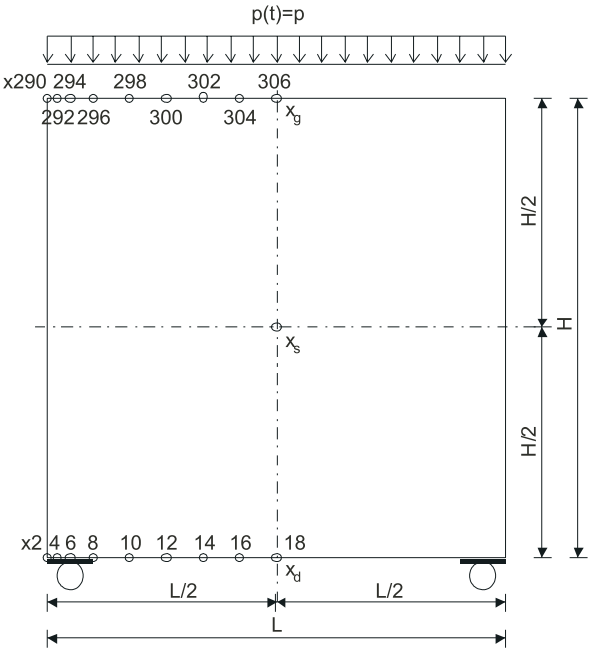

Fig. 4. Designation of points chosen for observation

In turn, the following points were selected for observation in order to illustrate the variability over time of the lower and upper edges of the deep beam:

— on the lower edge of the deep beam: x_2, x_4, x_6, x_8, x_{10}, x_{12}, x_{14}, x_{16}, x_{18},
— on the upper edge of the deep beam: x_{290}, x_{292}, x_{294}, x_{296}, x_{298}, x_{300}, x_{302}, x_{304}, x_{306},

the designations of which were shown in fig. 4.

In Fig. 5, for a *C100* concrete and A-III steel reinforced bean, the variability in time is presented of the vertical displacement of the selected points in the middle cross-section: point x_d — on the lower edge — Fig. 5_1, point x_s — half beam height — Fig. 5_2, point x_g — on the upper edge — Fig. 5_3, under various loads $\alpha = P/P_0$.

On the level of load $\alpha = 0.6$, a lack of stabilisation of plastic processes can be observed, which manifested itself at lower levels of load by a stabilised vibration around the permanent displacements of the observed points. Only during the initial phase of deformation of the deep beam, the symptoms of the oscillation of vertical displacement of point x_d around the point of balance could be observed. As a result, for the load level a = 0.6, an increase of vertical displacements of the observed points is visible, which signals load capacity depletion and the beam's damage.

In Fig. 6, for a *C200* concrete and A-III steel reinforced beam, the variability in time is presented of the vertical displacement of selected points in the middle cross-section: point x_d — on the lower edge — Fig. 6_1, point x_s — half beam height — Fig. 6_2, point x_g — on the upper edge — Fig. 6_3, under various loads $\alpha = P/P_0$.

At the load level of $\alpha = 0.6$, (like in the *C100* concrete deep beam), a lack of stabilisation of plastic processes was observed and manifested as a lack of stabilised vibration around the observed points' permanent displacements. As a result, the load level of $\alpha = 0.5$ determines the beam's load capacity.

In Fig. 7, for the *C300* concrete and A-III steel reinforced beam, the variability in time is presented of the vertical displacement of the selected points in the middle cross-section: point x_d — on the lower edge — Fig. 7_1, point x_s — half beam height — Fig. 7_2, point x_g — on the upper edge — Fig. 7_3, under various loads $\alpha = P/P_0$.

At the load level of $\alpha = 0.6$, (like in the *C100* and *C200* concrete deep beams), a lack of stabilisation of plastic processes was observed and manifested with a stabilised vibration around the observed points' permanent displacements under lower loads. However, the process of vibration movement stability loss at this load level was distributed over time and progressed differently than in the *C100* and *C200* concrete deep beams.

In Fig. 8, for a *C100* concrete and A-H steel reinforced beam, the variability in time is presented of the vertical displacement of selected points in the middle cross-section: point x_d — on the lower edge — Fig. 8_1, point x_s — half beam height — Fig. 8_2, point x_g — on the upper edge — Fig. 8_3, under various loads $\alpha = P/P_0$.

At load level $\alpha = 0.6$, a further development of stable plastic processes different from the case of the deep beam reinforced with *A-III* steel (for the same load level) can be observed, which was manifested by stabilised vibrating motion around permanent displacements of observed points. Unlike the case of the deep beam reinforced with *A-III* steel, at load level $\alpha = 0.7$, a lack of stabilisation of plastic processes can be observed, which manifested itself at lower loads with a stabilised vibration around the observed points' permanent displacements.

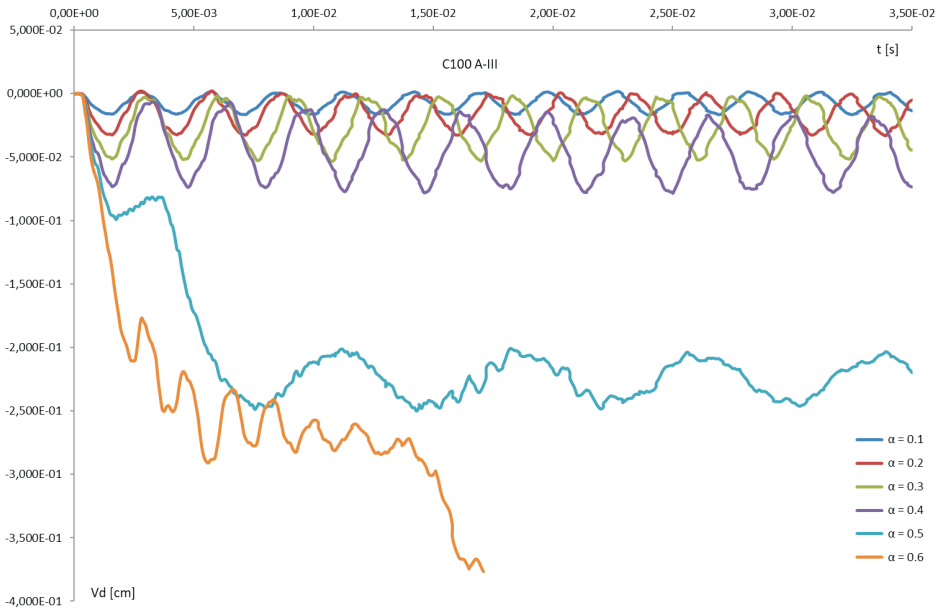

Fig. 5_1. Change in time of vertical displacement of point x_d in the middle cross-section on the beam's lower edge

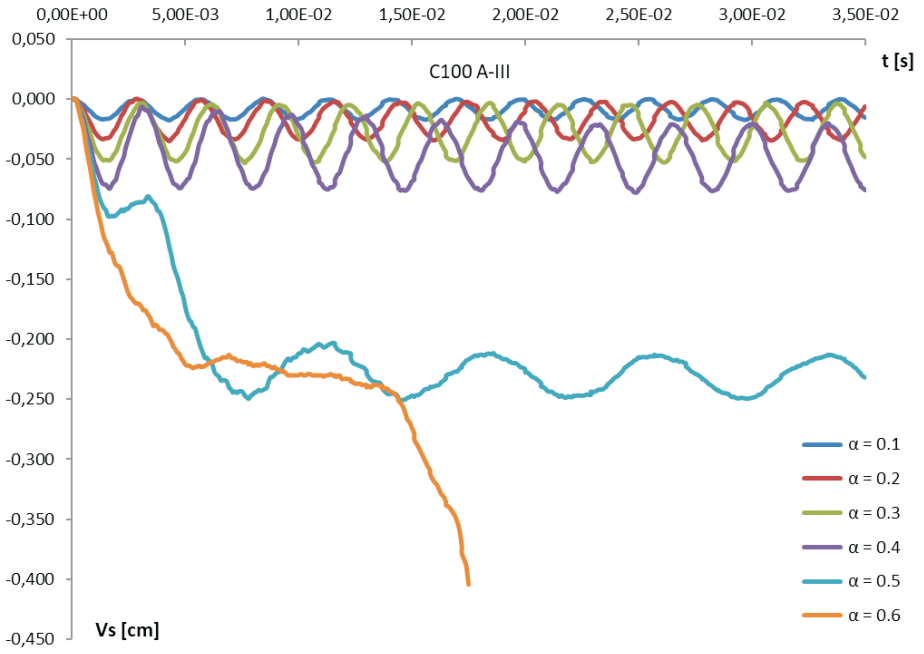

Fig. 5_2. Change in time of vertical displacement of point x_s in the middle cross-section at half of the beam's height

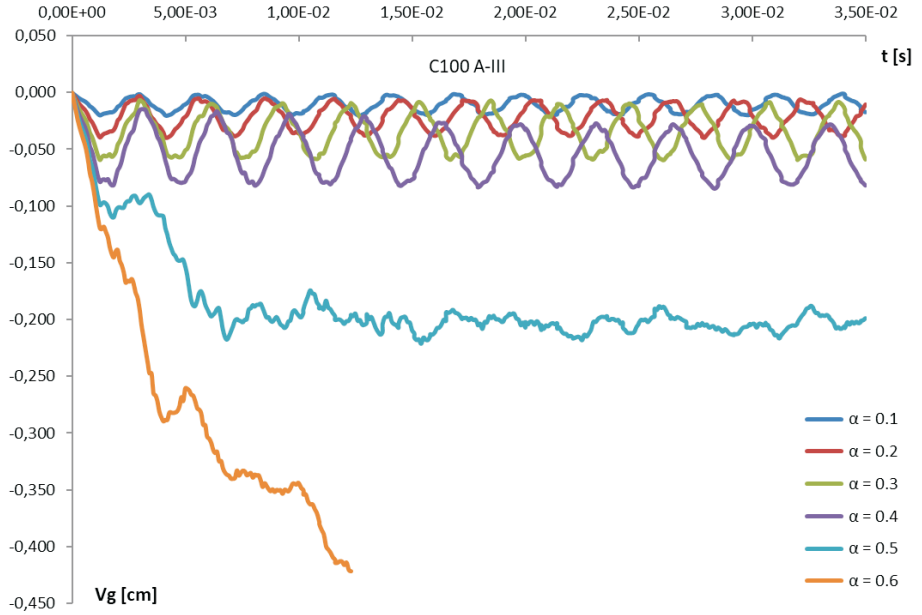

Fig. 5_3. Change in time of vertical displacement of point x_g in the middle cross-section on the beam's upper edge

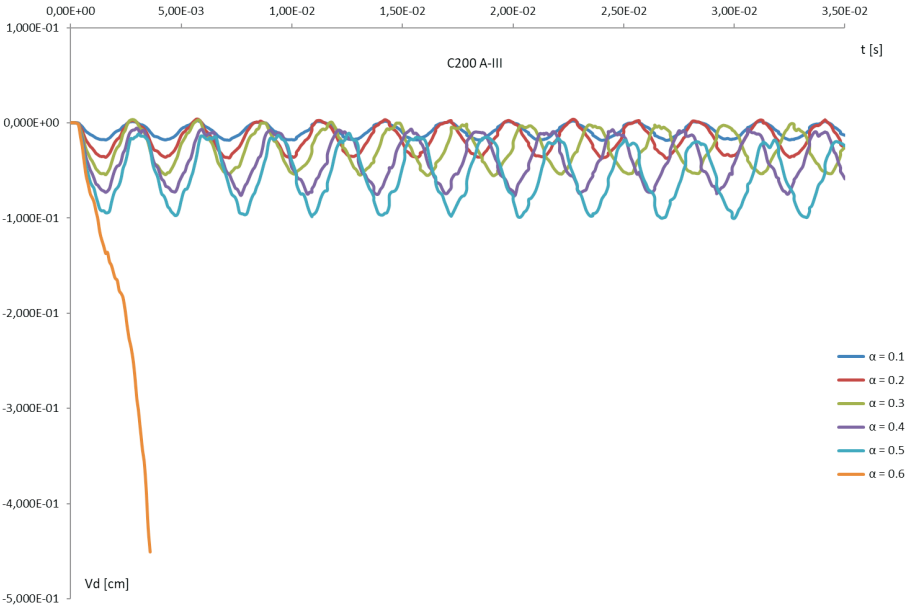

Fig. 6_1. Change in time of vertical displacement of point x_d in the middle cross-section on the beam's lower edge

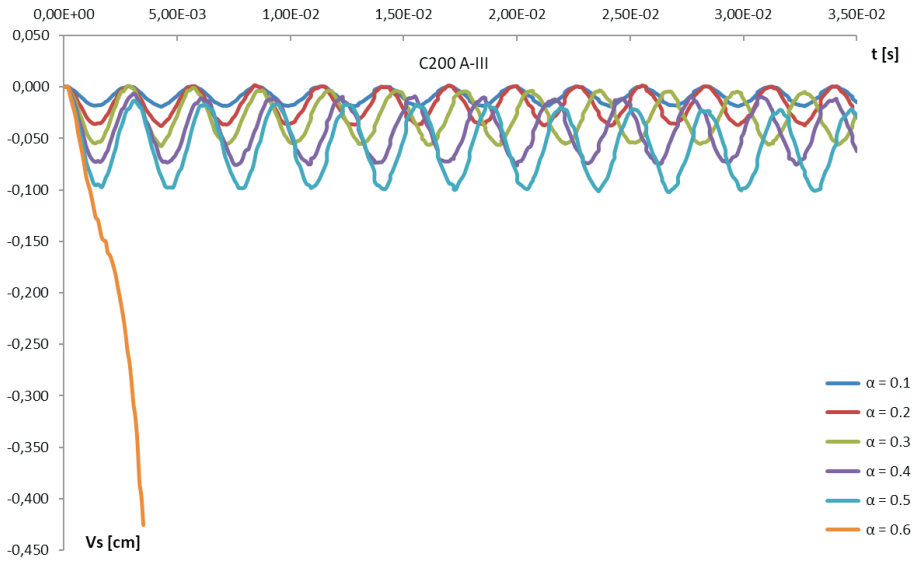

Fig. 6_2. Change in time of vertical displacement of point x_d in the middle cross-section at half of the beam's height

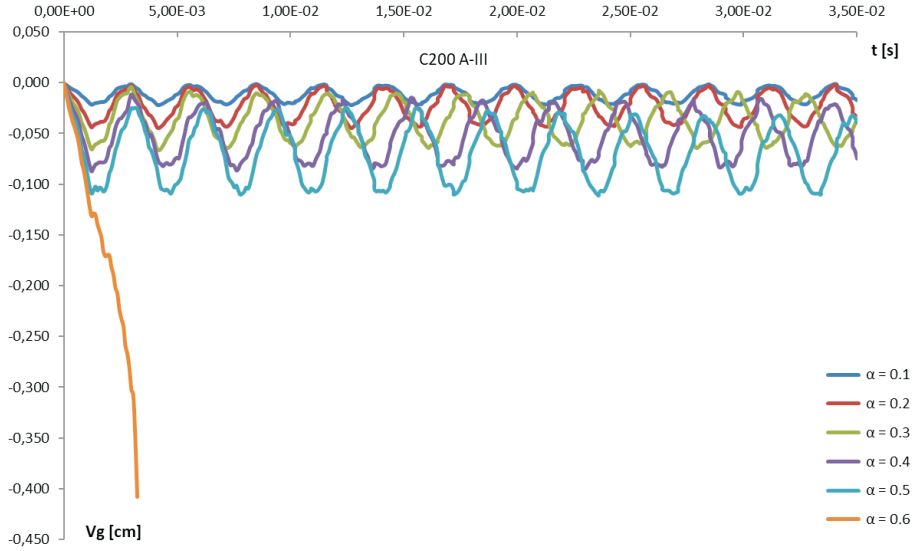

Fig. 6_3. Change in time of vertical displacement of point x_g in the middle cross-section on the beam's upper edge

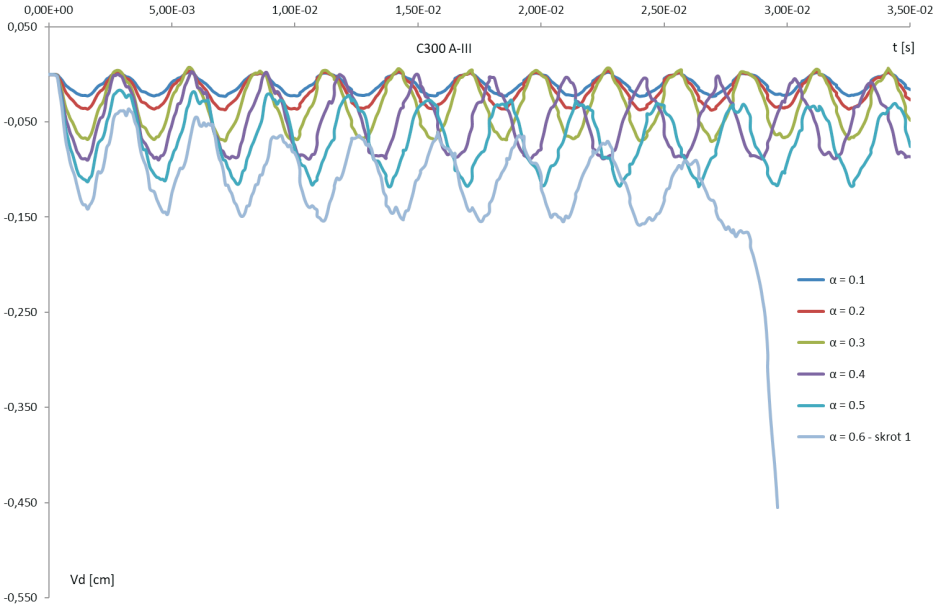

Fig. 7_1. Change in time of vertical displacement of point x_d in the middle cross-section on the beam's lower edge

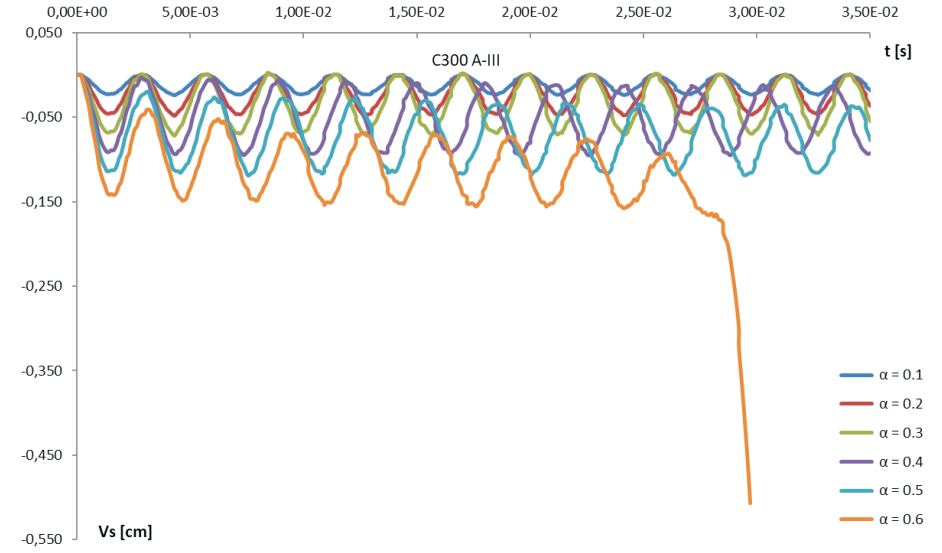

Fig. 7_2. Change in time of vertical displacement of point x_s in the middle cross-section at half of the beam's height

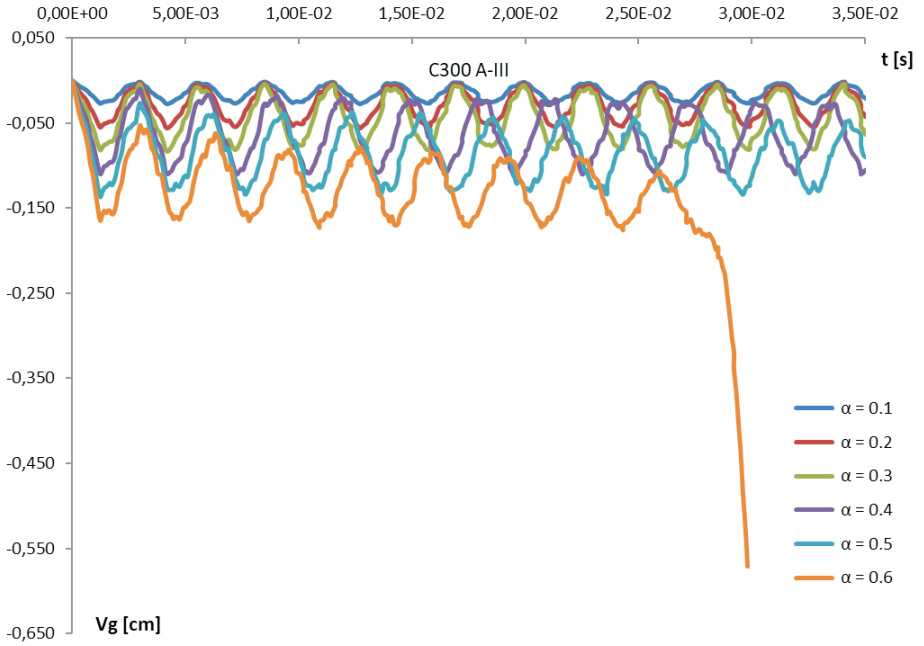

Fig. 7_3. Change in time of vertical displacement of point x_g in the middle cross-section on the beam's upper edge

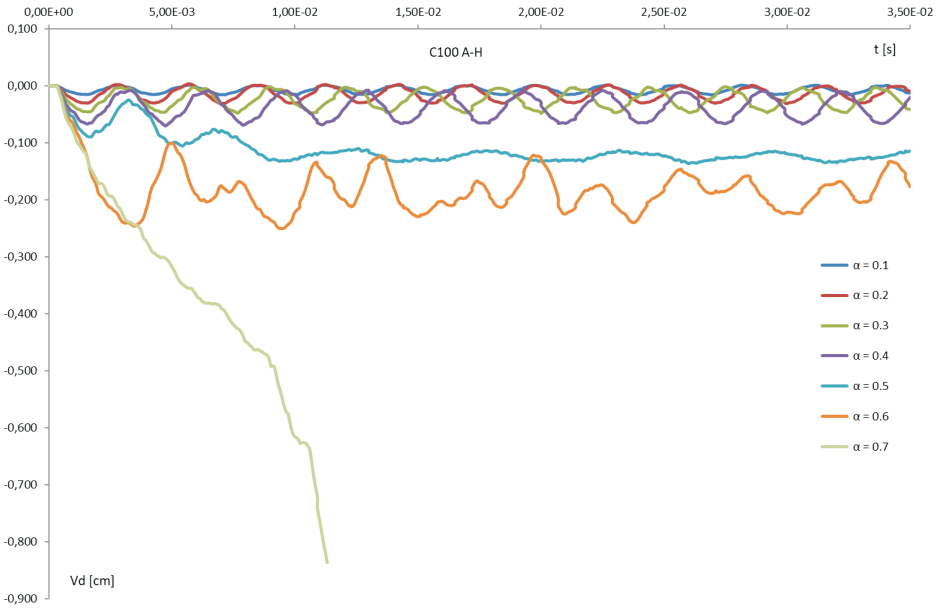

Fig. 8_1. Change in time of vertical displacement of point x_d in the middle cross-section on the beam's lower edge

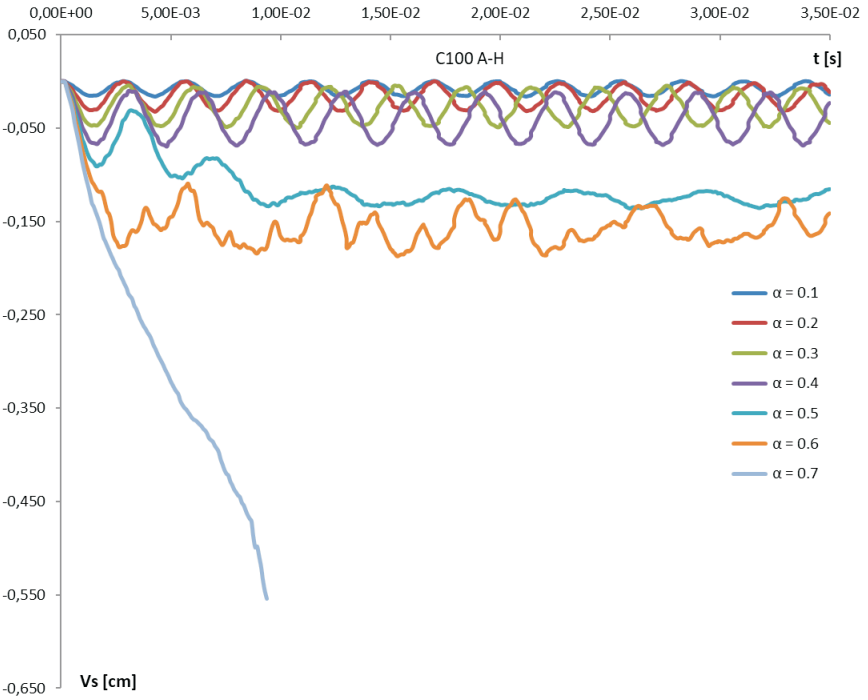

Fig. 8_2. Change in time of vertical displacement of point x_s in the middle cross-section at half of the beam's height

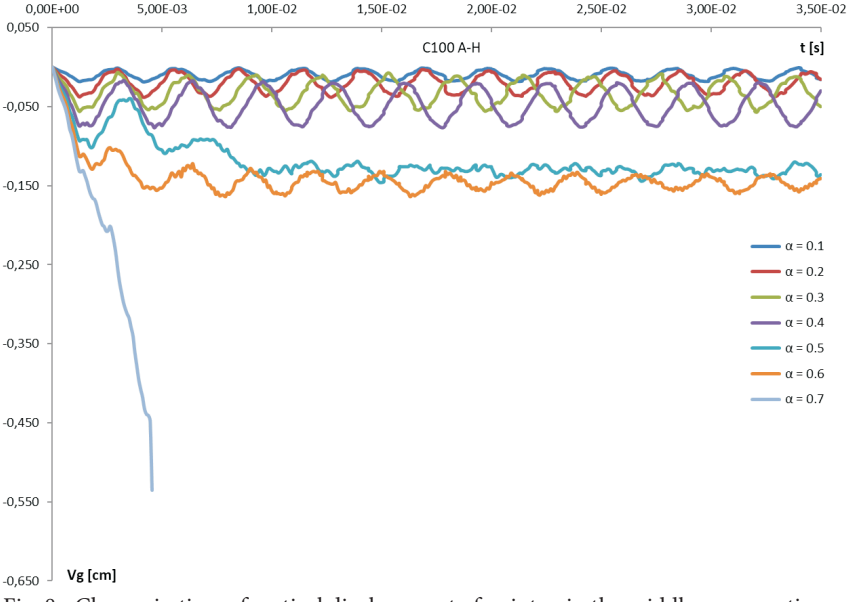

Fig. 8_3. Change in time of vertical displacement of point x_g in the middle cross-section on the beam's upper edge

In Fig. 9, for a *C200* concrete and A-H steel reinforced beam, the variability in time is presented of the vertical displacement of selected points in the middle cross-section: point x_d — on the lower edge — Fig. 9_1, point x_s — half beam height — Fig. 9_2, point x_g — on the upper edge — Fig. 9_3, under various loads $\alpha = P/P_0$.

Already at the load $\alpha = 0.5$, unlike for the *A-III* steel reinforced beam, the beam lost its loading capacity. The maximum load level was changed by the replacement of reinforcing steel grade *A-III* with grade *A-H*.

In Fig. 10, for a *C300* concrete and A-H steel reinforced beam, the variability in time is presented of the vertical displacement of selected points in the middle cross-section: point x_d — on the lower edge — Fig. 10_1, point x_s — half beam height — Fig. 10_2, point x_g — on the upper edge — Fig. 10_3, under various loads $\alpha = P/P_0$.

At the load level of $\alpha = 0.6$, like in the *A-III* steel reinforced deep beam, a lack of stabilisation of plastic processes was observed and manifested with a stabilised vibration around the observed points' permanent displacements under lower loads. However, the process of vibrating motion stability loss was more violent than in the deep beam reinforced with *A-III* steel.

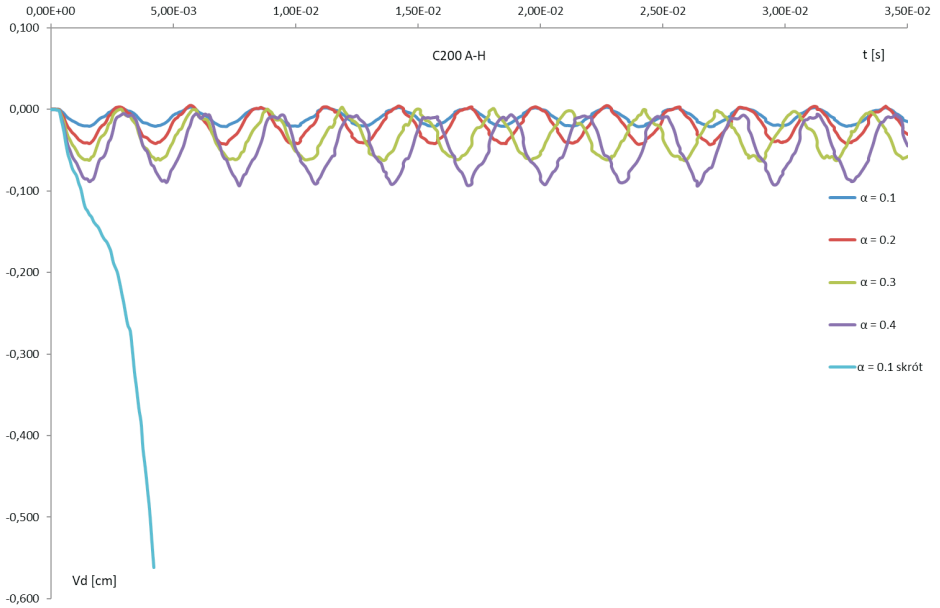

Fig. 9_1. Change in time of vertical displacement of point x_d in the middle cross-section on the beam's lower edge

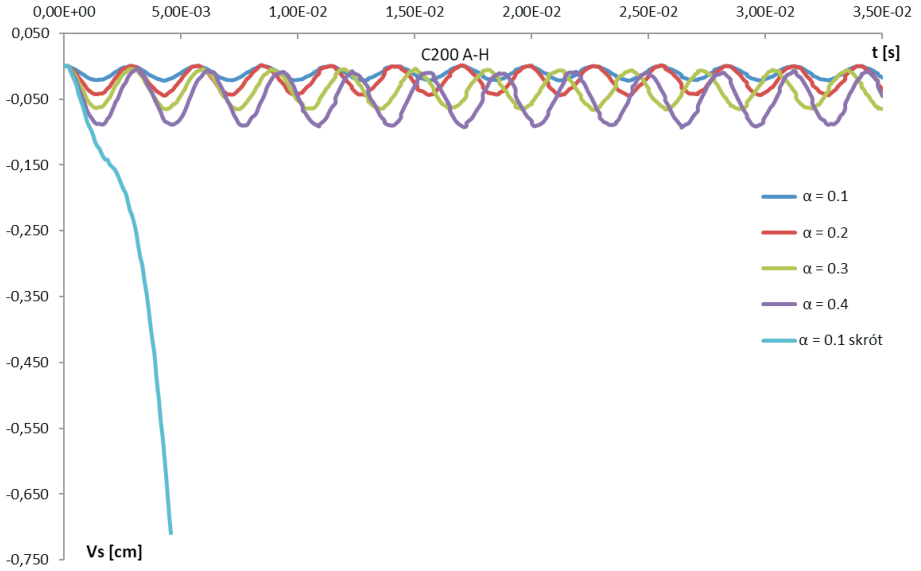

Fig. 9_2. Change in time of vertical displacement of point x_s in the middle cross-section at half of the beam's height

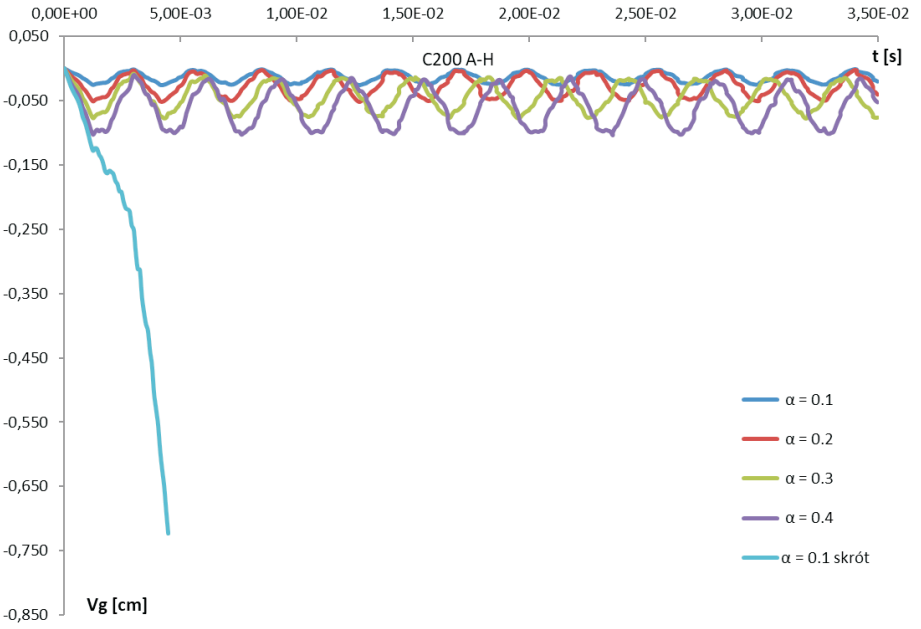

Fig. 9_3. Change in time of vertical displacement of point x_g in the middle cross-section on the beam's upper edge

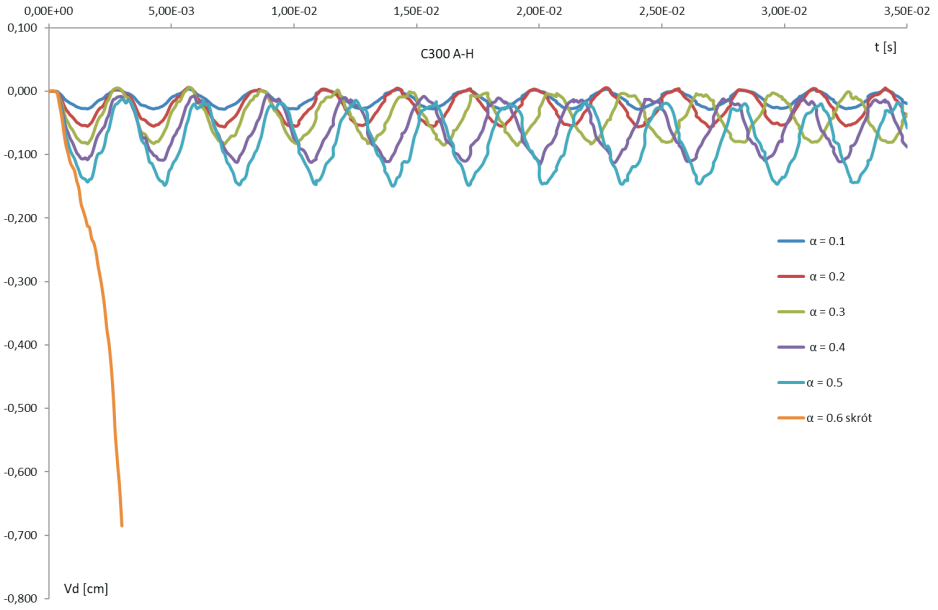

Fig. 10_1. Change in time of vertical displacement of point x_d in the middle cross-section on the beam's lower edge

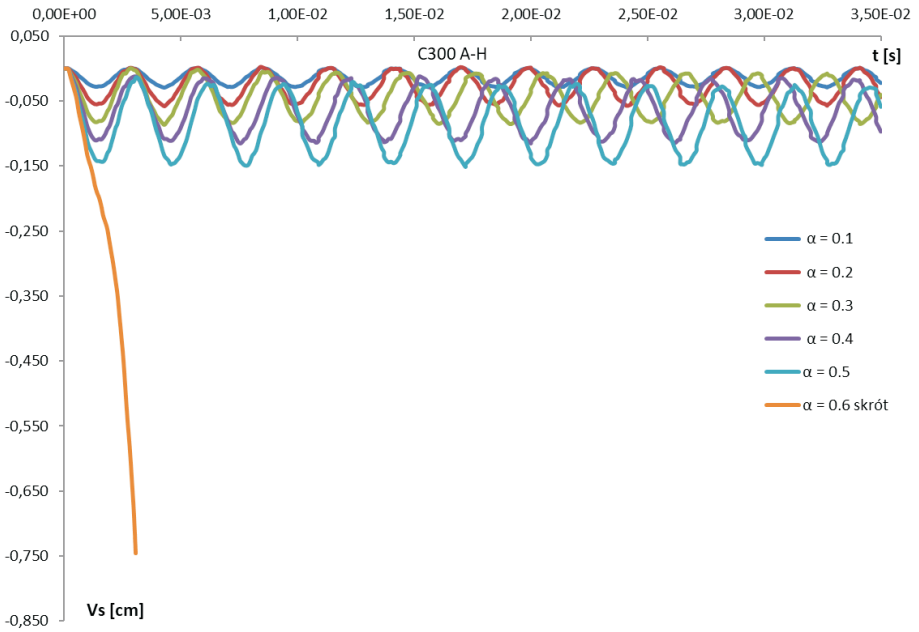

Fig. 10_2. Change in time of vertical displacement of point x_s in the middle cross-section at half of the beam's height

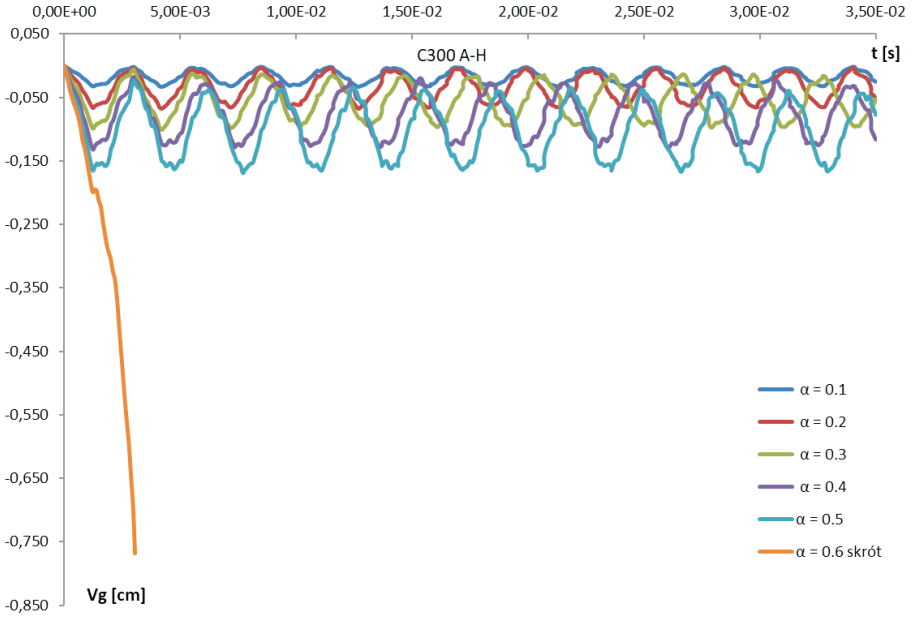

Fig. 10$_3$. Change in time of vertical displacement of point x_g in the middle cross-section on the beam's upper edge

3. Conclusion

The study has analysed the deformation of a rectangular reinforced concrete deep beam made of very high strength concrete of *C100, C200* and *C300* grades and reinforced with plain steel *A-III* and with high strength steel *A-H*, dynamically loaded. The differentiated process of dynamic stress/strain and deformation of the reinforced concrete deep beam has been described based on observation of changes in vertical displacement of points selected on the beam's lower and upper edges in its middle cross-section. As part of the analysis, it was established that increasing the strength of either concrete or steel can affect the reinforced concrete beam stress/strain and damage mechanisms by a differentiated process of concentration and changes of concrete matrix crack areas. The presented results confirmed it is necessary to investigate the effect of the constitutive model parameters of the very high-strength concrete and the increased-strength steel on the effort mechanism of reinforced concrete elements. A complete analysis of the impact of the analysed factors will allow the assessment of the desirability of designing such elements using a very high strength concrete as well as high strength steel. The results presented in this paper confirmed the correctness of the assumptions and deformation models of concrete and steel as well as the effectiveness of the methods of analysis proposed

for the problems of numerical simulation of the dynamic behaviour of reinforced concrete deep beams under dynamic loads.

The study was carried out as a result of research tasks carried out within the framework of statutory research no 934, carried out in the Faculty of Civil Engineering and Geodesy of the Military University of Technology.

Received February 26, 2018. Revised July 3, 2018.

Paper translated into English and verified by company SKRIVANEK sp. z o.o., 22 Solec Street, 00-410 Warsaw, Poland.

REFERENCES

[1] Cichorski W., Stolarski A., *Modelling of inelastic behaviour of reinforced concrete deep beam*, Journal of Achievements in Materials and Manufacturing Engineering, 44, 1, 2016, 37-44.

[2] Cichorski W., Stolarski A., *Analizy stanu przemieszczenia niesprężystej tarczy żelbetowej obciążonej statycznie*, Biuletyn WAT, 50, 5, 2001, 5-20.

[3] Cichorski W., Stolarski A., *Analizy wytężenia tarczy żelbetowej z materiałów konstrukcyjnych bardzo wysokich wytrzymałości*, Biuletyn WAT, 65, 4, 2016, 143-165.

[4] Kamińska M.E., Miszczak J., *Experimental and analytical aspects of HSC confinement in tied slender columns*, 3rd International Conference on Analytical Models and New Concepts in Mechanics of Concrete Structures, Wrocław – Świeradów Zdrój, Poland, June 16-19, 1999, 109-114.

[5] Kleiber M., *Metoda elementów skończonych w nieliniowej mechanice kontinuum*, PWN, Warszawa, 1985.

[6] Leonhardt F., Walther R., *Wandartige träger*, Report, Deutscher Asschüb für Stahlbeton, 229, Germany, Berlin, 1966.

[7] Lewiński P.M., *Nieliniowa analiza płyt i tarcz żelbetowych metodą elementów skończonych*, PWN, Warszawa-Łódź, 1990.

[8] Majorama C.E., Salomoni V.A., Schrefler B.A., *A constitutive relationship for high performance and ultra high performance concrete*, The Euro-C 1998 Conference on Computational Modelling of Concrete Structures, Badgastein, Austria, 31 March – 3 April 1998, 1, 203-208.

[9] Marzec I., Tejchman J., Winnicki A., *Computational simulations of concrete behaviour under dynamic conditions using elasto-visco-plastic model with non-local softening*, Computers & Concrete, 15, 4, 2015, 515-545.

[10] Miedziałowski Cz., *The static and dynamic analysis of building structures. Selected problems*, Oficyna Wydawnicza Politechniki Białostockiej, 2015.

[11] Ožbolt J., Meštrović D., Li Y.J., Elighausen R., *Compression Failure of Beams Made of Different Concrete Types and Sizes*, Journal of Structural Engineering, 126, 2, 2000, 200-209.

[12] Rashid M.A., Mansur M.A., *Reinforced high-strength concrete beams in flexure*, ACI „Structural Journal", vol. 102, no. 3, 2015, 462-471.

[13] Stolarski A., *Dynamic strength criterion for concrete*, Journal of Engineering Mechanics, ASCE, vol. 130, 12, 2004, 1428-1435.

[14] Stolarski A., *Model dynamicznego odkształcania betonu*, Archiwum Inżynierii Lądowej, 37, 3-4, 1991, 405-447.

[15] Stolarski A., Cichorski W., *Modelowanie statycznego i dynamicznego zachowania tarcz żelbetowych*, Komitet Inżynierii Lądowej i Wodnej PAN, Studia z Zakresu Inżynierii, 51, Warszawa, 2002.

[16] Stolarski A., Cichorski W., *Influence of high strength of concrete and reinforced steel on dynamic behavior of reinforced concrete deep beams*, Proceedings of the 12rd International Conference on Shock & Impact Loads on Structures, Singapore, 15-16 June 2017, 159-168.

[17] Stolarski A., Cichorski W., *Oszacowanie nośności tarczy żelbetowej z uwzględnieniem betonu bardzo wysokiej wytrzymałości*, Biuletyn WAT, 51, 2, 2002, 49-67.

[18] Winnicki A., Pearce C.J. and Bićanić N., *Viscoplastic Hoffman consistency model for concrete*, Comput. & Struct., 2001, 79, 7-19.

WALDEMAR CICHORSKI

Analiza stanu przemieszczenia tarcz żelbetowych z betonów o bardzo wysokiej wytrzymałości obciążonych dynamicznie

Streszczenie. W pracy przedstawiono analizę deformacji prostokątnych tarcz żelbetowych wykonanych z betonów o bardzo wysokiej wytrzymałości obciążonych dynamicznie z uwzględnieniem fizycznych nieliniowości materiałów konstrukcyjnych: betonu i stali zbrojeniowej. Rozwiązanie otrzymano na podstawie metody zaprezentowanej w pracy [15]. Dokonano analizy stanu przemieszczenia dla trzech rodzajów tarcz, przy różnych poziomach obciążenia, aż do osiągnięcia stanu wyczerpania dynamicznej nośności. Przedstawiono wyniki rozwiązań numerycznych ze szczególnym uwzględnieniem wpływu bardzo wysokiej wytrzymałości betonu i stali na przemieszczenia tarczy żelbetowej. Wykazano poprawność przyjętych założeń i modeli odkształcenia betonu i stali oraz efektywność metody analizy proponowanej w pracy [1, 15] dla problemów numerycznej symulacji zachowania tarcz żelbetowych.
Słowa kluczowe: mechanika konstrukcji, konstrukcje żelbetowe, tarcze, obciążenie dynamiczne, nieliniowość fizyczna
DOI: 10.5604/01.3001.0012.6612